WILEY | Hindawi

*Retraction*

# Retracted: Research on the Characteristics of Surface Flux and Surface Parameters of Meadow Underlying Surface in the Source Region of Yellow River

## Security and Communication Networks

This article has been retracted by Hindawi, as publisher, following an investigation undertaken by the publisher [1]. This investigation has uncovered evidence of systematic manipulation of the publication and peer-review process. We cannot, therefore, vouch for the reliability or integrity of this article.

Please note that this notice is intended solely to alert readers that the peer-review process of this article has been compromised.

Wiley and Hindawi regret that the usual quality checks did not identify these issues before publication and have since put additional measures in place to safeguard research integrity.

We wish to credit our Research Integrity and Research Publishing teams and anonymous and named external researchers and research integrity experts for contributing to this investigation.

The corresponding author, as the representative of all authors, has been given the opportunity to register their agreement or disagreement to this retraction. We have kept a record of any response received.

## References

[1] Q. Luo, T. Zhang, Z. Li, and J. Yang, "Research on the Characteristics of Surface Flux and Surface Parameters of Meadow Underlying Surface in the Source Region of Yellow River," *Security and Communication Networks*, vol. 2022, Article ID 2088858, 11 pages, 2022.

WILEY | Hindawi

*Research Article*

# Research on the Characteristics of Surface Flux and Surface Parameters of Meadow Underlying Surface in the Source Region of Yellow River

**Qi Luo [1,2] Tinglong Zhang,[1,2] Zhenchao Li,[3] and Jing Yang[2,4]**

[1]*Hainan Institute of Meteorological Sciences, Haikou, China*
[2]*Key Laboratory of South China Sea Meteorological Disaster Prevention and Mitigation of Hainan Province, Haikou, China*
[3]*Key Laboratory of Land Surface Process and Climate Change, Northwest Institute of Eco-Environment and Resources CAS, Lanzhou, China*
[4]*Hainan Climate Center, Haikou, China*

Correspondence should be addressed to Qi Luo; qluo1987@stu.ahu.edu.cn

Based on observation data from January 1st to December 31st in 2014 at Maduo Site, which is located near the Yellow River source area in the Qinghai-Tibet Plateau, this research examined how the surface flow of alpine meadow underlying surface varies. The applicability of the land-surface process models CLM5.0 and CLM4.5 in alpine grassland was also tested. The findings revealed that total radiation in the Yellow River source area was lower in the winter but quickly increased after mid-March, peaked in June or July, and then gradually decreased. The surface reflected radiation was affected by both the total radiation and surface albedo. Its seasonal variation showed different characteristics than the total radiation. Due to the snow on the surface, the short-wave radiation reflected by the surface was larger in winter, while the surface reflected radiation in summer was relatively small, especially after the rainy season. Long-wave surface radiation followed the same seasonal pattern as air counter radiation, with a low point in winter and a high point in summer. Due to cloud cover and other variables, however, long-wave surface radiation was larger than atmospheric counter radiation. The sensible heat flux and net radiation varied similarly until July (rainy season), but after July, the latent heat flux and net radiation followed the same pattern until the soil was frozen in early November. For the whole year, the study of regional surface flux was mainly focused on latent heat flux. Corresponding to sensible heat and latent heat, the daily average of soil heat flux was above 0 from mid-March to late August, which meant that the soil heat flux was transmitted from the surface soil to the deep layer, while the rest of the time showed a negative, with soil heat flux transmitted from the deep layer to the surface soil. In late March, the daily average heat flux of soil was abnormally large, which was related to the melting of frozen soil. Generally, for the whole year, soil heat flux was transmitted from the deep layer to the surface soil. The simulation results of CLM5.0 and CLM4.5 for radiation flux and surface heat flux are very close to the observed values, especially CLM5.0. This indicates that the simulation effect of the model in Alpine Grassland in the source region of the Yellow River has been significantly improved after improving many parameterization schemes and dynamic processes in CLM5.0. However, the soil freezing and thawing process and snow parameterization scheme in CLM need to be further improved. Generally, the daily average $CO_2$ flux during the frozen period of soil was 0. In May, September, and October, the respiration of alpine meadows dominated, surface releasing $CO_2$, while in early and middle June, photosynthesis played the leading role, surface absorbing $CO_2$. During the period from late June to mid-August, when both the moisture and temperature of soil were higher, and the surface vegetation experienced rapid growth, the daily average $CO_2$ flux increased sharply. On the contrary, when the frozen soil melted, the $CO_2$ flux released by the surface increased significantly.

## 1. Introduction

The land-surface process serves as an important part of the Earth science system and determines the matter-energy exchange characteristics between the land-surface and the atmosphere. In that way, it profoundly affects the global atmospheric circulation and regional weather and climate. In recent years, the land-surface process, together with its interactions with climate, has caused widespread concerns in human society and has gradually become an important focus of scientific research. [1] Dickinson (1995) pointed out in the report of the American Geophysical Union that improving the Land-Surface Process Model, which was coupled with the atmospheric model, was one of the main ways to lift the forecasting ability of the numerical model. However, the research on PIPLS showed (Henderson [2], 1993) that a great many uncertainties existed in the surface flux simulation of the current Land-Surface Process Model, which would result in a considerable deviation of flux transport. As a result, conducting in-depth studies on the physical and biochemical processes of various underlying surfaces interacting with the atmosphere has become an urgent need for research on global climate change and global change in order to continuously improve and develop the Land-Surface Process Model, make it more similar to the real situation, and predict various exchange processes such as momentum, energy, and matter as accurately as possible (Sun [3], 2005). However, the development of the Land-Surface Process Model must be supported by important basic data.

It is an important approach to optimizing the simulation performance of weather and climate models through analysis of observation data, which would gradually enhance the understanding of how energy and matter exchange between the land and the atmosphere and then revise the parameters and parameterization involved in the land-surface process. The surface energy exchange based on surface heat balance and radiation balance is the main part of the land-atmosphere interaction. It serves as an energy tie in the land-atmosphere coupling process and also an essential link in the Earth system's solar energy transformation as well as heat and water circulation. This process has a significant impact on the energy balance of different ecosystems, greatly determining the local climate characteristics (Heusinkveld [4], 2004). The effects of solar activity, vegetation growth, and human and other factors on climate change are mainly realized through changes in surface heat and radiation balance, and their response to climate change is also conveyed through processes such as surface heat transfer. Therefore, research on the characteristics of surface heat change has been a focus of great concern in the study of global change and climate anomalies. Whether the simulation of surface heat and radiant flux is accurate is often the main indicator in the simulation performance evaluation of the Land-Surface Process Model. It is of great scientific significance to study the surface flux of different underlying surfaces.

The source area of the Yellow River is located in the northeast of the Qinghai-Tibet Plateau, where there are diversified landforms, such as mountains, basins, canyons, grasslands, lakes, swamps, glaciers, and wetlands and widely distributed permafrost. It is an important water conservation area in China and an important part of the Sanjiangyuan National Nature Reserve. This area is a typical case of the complex lake-alpine meadow underlying surface. The land-atmosphere interaction there not only directly affects the climate and environmental change of the Qinghai-Tibet Plateau but also greatly affects that of East Asia and the world. Therefore, it is of great significance for the development of both model and community economy to thoroughly understand the characteristics of surface flux and surface parameters in this region because it would help improve the simulation accuracy of the Land-Surface Process Model for this place, thereby enhancing the simulation capability of Climate System Model and underpinning the regional climate and environment evaluation.

At present, there have been many studies on the land-surface process of the Yellow River source area and even of the entire Qinghai-Tibet Plateau ([5–8] Tanaka et al., 2001; Yao et al., 2011; Li et al., 2014; Gu et al., 2015), but due to data limitation, the previous research mainly focused on the analysis of a certain aspect or specific parameters of the land-surface process, failing to reflect the overall characteristics of the land-surface process in the Yellow River source area. Therefore, this paper intends to use the observation data system to analyze the surface flux and land-surface parameters of the most widely distributed alpine meadow underlying surface in this region, with the aim of facilitating the improvement and development of the Land-Surface Process Model of Qinghai-Tibet Plateau, and providing a scientific basis for the protection of ecological environment together with the promotion of socio-economic development in the Yellow River source area.

This paper is organized as follows: Section 2 presents an introduction of observational data and land process models. Section 3 describes the results and discussions; Section 4 summarizes this paper and offers directions for future work.

## 2. Introduction of Observational Data and Land Process Models

*2.1. An Overview of the Research Area and Observation Data.* The research area is located in Maduo County and Qumalai County of Qinghai Province in the Yellow River source area, between 96.6 and 98.4°E and 34.3–35.5°N and one hour later than Beijing time. As most of the area is 4100–4500 m above sea level, lakes scatter widely, among which Eling Lake is the largest one at the source of the Yellow River, with an area of 610 km$^2$, water storage capacity of about $107.6 \times 108$ m$^3$, the average water depth 17.6 m and maximum water depth 30.7 m. The latitude and longitude of the field observation site are 97°33′12.51″E, 34°54′47.25″N, respectively, which is located on the grassland about 1.5-2 km west of the Eling Lake. The altitude is 4280m, and the vegetation height of the observation site is about 5–10 cm. The specific location of the observation site and the condition of the underlying surface are shown in Figure 1. A set of eddy-related systems was set up in the experiment, containing a three-dimensional
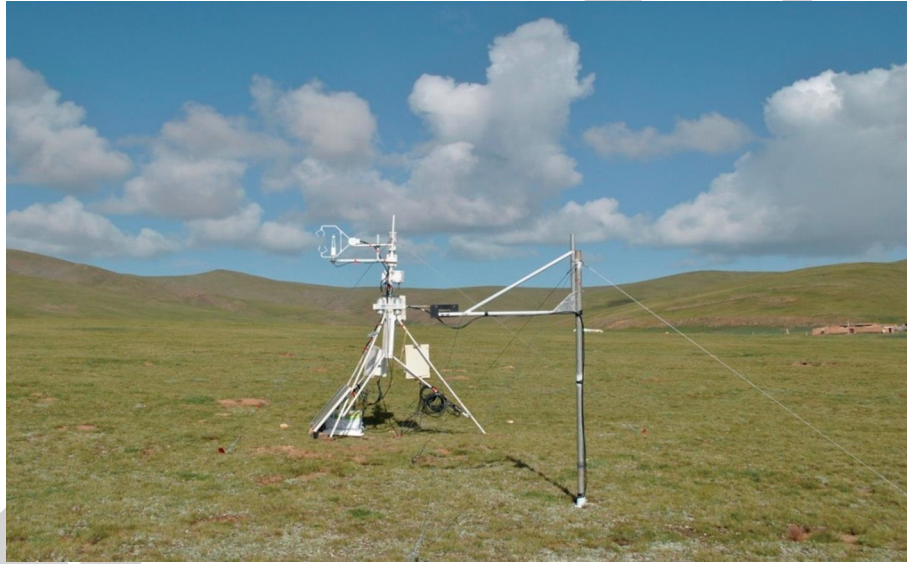
(a)



(b)
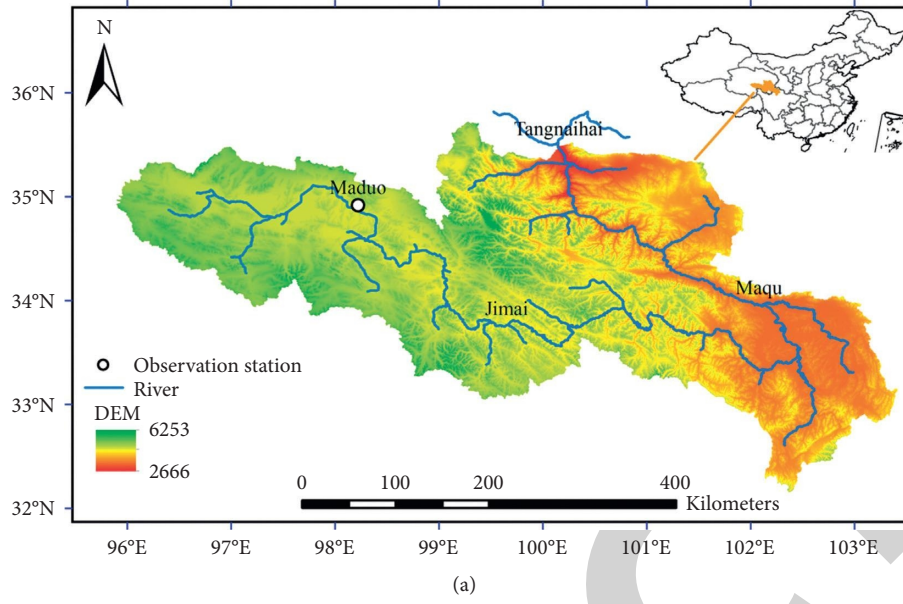
Figure 1: (a) The position of the observation site and (b) the condition of the underlying surface.

ultrasonic anemometer (CSAT3, Campbell, USA), an open-circuit CO2/H2O gas analyzer (LI-7500, LI-COR, USA), and a data collector (CR3000 and CR5000, CSI, USA), with 10 Hz of sampling frequency. The observation height of turbulence flux, temperature, wind speed, air pressure, and other factors was 3.2 m, while that of CNR-1 net radiation (KIPP and ZONEN, Netherlands) was 1.5 m. HMP45 C air temperature and humidity sensor (Vaisala, Finland) was applied to the measurement of air temperature. The burial depths for soil temperature and humidity measurement were 0.05, 0.10, 0.20, 0.40, 0.80, 1.60, 3.20 m, respectively, and the instruments applied were, respectively, 107 thermistor temperature probe and CS616 volumetric water content reflectometer from the American scientific instrument company, Campbell. As for the observation of two layers of soil heat flux, the instrument used was the HFP01 heat flux

plate from the Nether-landish thermal sensor company, Hukseflux, and the burial depths were 0.05 m and 0.2 m, respectively. The data period covered in this paper was from January 1st to December 31st, 2014.

In order to improve the accuracy of data, the research has conducted quality control over the eddy observation data, including abnormal data deletion, ultrasonic temperature correction of sensible heat flux, WPL correction of water vapor, and carbon dioxide flux. This research has eliminated the data that was obviously abnormal (mainly due to data anomalies and missing data caused by rain and snow), and the missing data was supplemented by interpolation [9–14].

In this paper, the daily average data were used to analyze the seasonal variation characteristics of surface flux and land-surface parameters of meadow underlying surface in the Yellow River source area, and January, April, July, and

October were adopted to represent the four seasons, i. e., winter, spring, summer, and autumn, respectively. Specifically, the monthly average of each representative month was used to analyze the daily characteristics of surface flux in each season. In order to reduce the error, the short-wave radiation was analyzed based on the daily data from 9 : 00 to 17 : 00.

*2.2. Introduction of the Land Process Model and Numerical Test.* CLM (community land model) is one of the most mature and applicable models. It integrates the advantages of the land-surface process model (LSM) of NCAR and biotransmission scheme model (bats) of the biosphere and makes corresponding parameterization improvements for some physical processes. CLM is a comprehensive surface model that can simulate Biophysics (such as radiative transfer, radiative transfer, radiative transfer, radiative transfer, and so on Energy fluxes and Hydrology) and biogeochemical processes (such as carbon and nitrogen dynamics). CLM5.0 is the latest version of CLM, which was released in February 2018. Compared with the previous version clm4.5 (released in July 2013), CLM 5.0 largely modifies the vegetation related processes. It uses Medlyn stomatal conductance model (Medlyn et al. 2011) instead of the ball berry stomatal conductance model (Collatz et al. 1991). It abandons the previous simple calculation method of plant water stress based on soil water potential and adopts a plant hydraulics scheme to explain the different water potential of leaf, stem, root, and soil. CLM 5.0 increases the soil dry layer and significantly reduces soil evaporation, which is usually overestimated in earlier versions of CLM (Swenson and Lawrence, 2014).

This study uses the 2014 forced data-driven numerical model from the CLM default global forcing data (crucep). The temperature of Maduo site collected from global products is quite compatible with Maduo site data in 2014, with a correlation coefficient greater than 0.95. Other forcing variables are also similar to the observed values. In the simulation, the observation site of Maduo grassland was set as 30% wetland and 70% vegetation, and the soil texture was 30% clay, 33% silt, and 37% sand. In order to reduce the impact of initial field uncertainty on the simulation results, the crucep data in 2014 was forced to run for 300 years, and the simulation was taken as spin up to ensure that the surface variables entered a stable state (Yang et al. 1995).

## 3. Results and Discussion

*3.1. 5 cm Soil Temperature and Humidity.* Soil moisture, which is an important physical quantity in climate change research, has been drawing the attention of relevant research. Its importance stems from its capacity to affect climate change by altering surface albedo, soil thermal conductivity, and the amount of sensible and latent heat carried to the atmosphere. Furthermore, the release or absorption of heat by the phase change of soil moisture has a significant impact on heat transport in soil. Therefore, before analyzing the surface flux and surface parameters of the research area, it is necessary to analyze the near-surface soil temperature and soil moisture there. Figure 2 shows the trend of daily average soil temperature (a) and soil moisture (b) of 5 cm depth from January 1st to December 31st, 2014. It can be seen from the figure that due to the high altitude, the daily average soil temperature of the Yellow River source area was below 0°C from January to March, when the soil was frozen, and that of the period from the beginning of April to mid-October was above 0°C, with the peak occurring in July and then gradually retreating to negative after mid-October. On the other hand, the daily average soil moisture of 5 cm depth was relatively smaller during the frozen period of soil, and the volumetric water content was only 0.06 on average.

In late March, although the daily average soil temperature of 5 cm depth was still below 0°C, due to the daytime thawing and nighttime freezing, the daily average soil moisture of 5 cm depth started to rise. The period from the beginning of May to the middle of June marked relatively smaller soil moisture during the nonfrozen period. With the onset of the rainy season in late June, soil moisture grew rapidly and continued to rise until the end of October, when the daily average soil moisture might reach 0.32. The soil moisture of 5 cm depth fell fast after the freezing period began in early November. Although there was no precipitation data, it could be seen from Figure 2(b) that the research area experienced little precipitation before late June, as opposed to the abundant rainfall from the end of June to October.

The result of CLM simulating the variation trend of soil temperature and humidity is fairly good. 5 cm soil temperature is significantly affected by air temperature, and CLM can largely capture its fluctuation. However, the simulated value of soil temperature is lower than the observed value during the nonfreezing period from March to September. The annual root means a square error of CLM5.0 and CLM 4.5 is 5.4°C and 7.0°C, respectively. The fundamental reason for this is that the underlying surface of the Maduo site is significantly more intricate, and the model's soil state may differ from that of the Maduo site. The results demonstrate that during the period of soil freezing and thawing, the soil moisture predicted by CLM is much smaller than the measured value, with a root mean square error of 0.06. The main reason is that the shallow soil has the phenomenon of day thawing and night freezing, but the model cannot respond to the freezing and thawing process well, which indicates that the soil freezing and thawing process and snow parameterization scheme in the model need to be further improved.

*3.2. Radiation Flux.* Figure 3 shows the trend of daily average surface total radiation (DR), reflected radiation (UR), atmospheric counter radiation (DLR), and surface long-wave radiation (ULR) from January 1 to December 31, 2014. The total radiation in the study area was smaller in winter, with an average of about 420 W/m$^2$, but rose rapidly after mid-March, reaching a maximum in June or July with an average of about 650 W/m$^2$, and then slowly decreased.
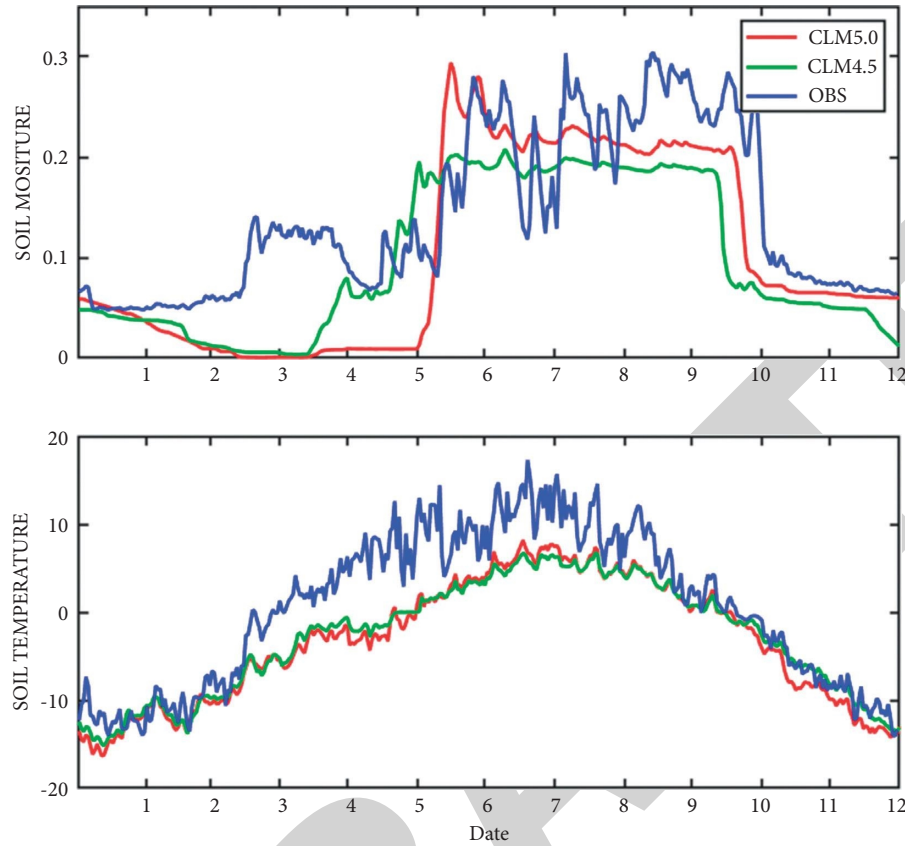
FIGURE 2: 5 cm Daily average variation of soil temperature (a) and soil moisture (b) at the source region of Yellow River (observed and simulated).
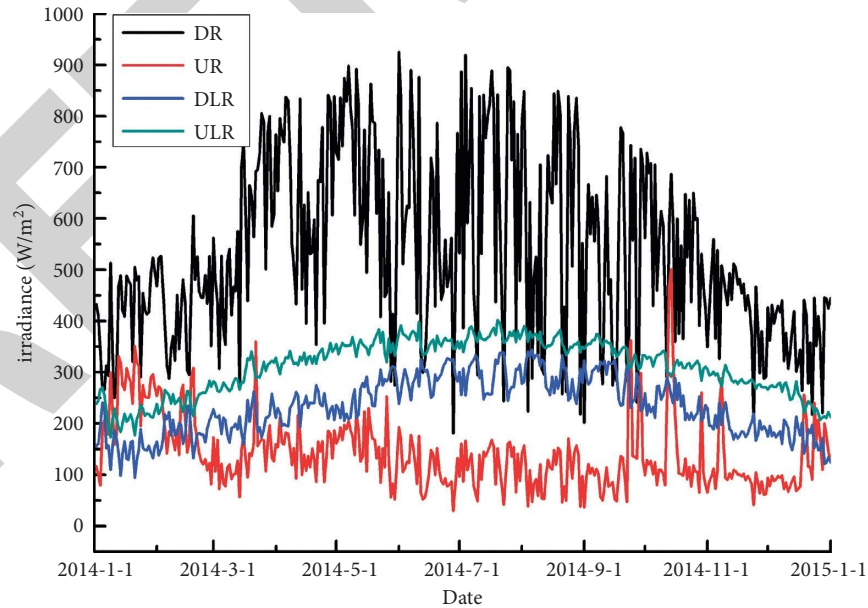


FIGURE 3: Daily average variation of surface radiation at source region of Yellow River, 2014.

Precipitation and cloud cover were two contributing elements that caused total radiation to fluctuate often. The solar elevation angle has the greatest impact on the seasonal variance in total radiation. The daily average of surface reflected radiation generally showed a trend consistent with that of the total radiation, which was increasing (decreasing) with the increase (decrease) of total solar radiation, but the seasonal trend of it was not the same as that of total

radiation. Due to the snow cover on the surface, the short-wave radiation reflected by the surface was generally larger in winter, and because of the high altitude and low temperature in the study area, there was snowfall in spring and autumn. Therefore, the short-wave radiation was reflected by the surface-displayed exceptional high values in spring and autumn. The surface reflected radiation in summer was smaller compared to other seasons, especially after the rainy season, which resulted from the increase in soil moisture, and the short-wave radiation reflected by the surface could be even smaller. Long-wave surface radiation has a similar seasonal fluctuation to air counter radiation, with a low point in winter and a high point in summer. The long-wave surface radiation, on the other hand, was greater than the air counter-radiation. In 2014, the long-wave surface radiation averaged about 311 W/m$^2$, while the atmospheric counter radiation was 234 W/m$^2$. Besides, due to factors such as cloud cover, the amplitude of daily average atmospheric counter radiation was greater than the daily average of long-wave surface radiation.

It can be seen from Figure 4 that the simulation results of CLM5.0 for radiation flux are obviously better than CLM4.5. CLM5.0 can well simulate the variation trend of radiation flux with a small error compared with the observed values, while CLM4.5 has a better simulation effect for reflected radiation, and the simulated values are all lower than the observed values. Total surface radiation varies substantially, and the CLM is unable to adequately reflect this variation. CLM4.5 replicates reflected radiation more accurately, whereas CLM5.0 better captures reflected radiation fluctuations. For surface long-wave radiation, the simulation results of CLM5.0 and CLM4.5 are both lower, which may be caused by the lower simulation results of soil temperature.

*3.3. Surface Heat Flux.* Figure 5 shows the trend of daily average surface net radiation (Rn), sensible heat (H), latent heat (LE), and soil heat flux of 5 cm depth from January 1 to December 31, 2014. As could be seen from the figure, the trend of daily average net radiation was similar to that of total radiation, which was rising rapidly after mid-March, reaching a maximum in July, and then slowly decreasing. During the study period, the effective surface radiation (long-wave surface radiation—atmospheric counter radiation) remained stable, and the net radiation was primarily governed by total radiation and surface albedo. Due to the smaller total radiation and larger surface albedo in winter, the net radiation reached the minimum in winter, even below 0 in January. Daily average net radiation rose rapidly in early July, which was directly related to the reduction in surface albedo caused by a sudden increase in soil moisture (Figure 2(b)) during this period. The sensible heat flux was generally negative in January 2014, rising slowly from February to May, reaching a maximum in May, and then slowly decreasing. On the other hand, the trend of latent heat flux was really different from that of sensible heat flux. In the first six months, when the soil moisture was low, the latent heat flux was small, but since early July, it had increased rapidly with the increase of soil moisture.

It was obvious based on the figure that before July, the sensible heat and net radiation generally showed a similar trend. However, after July, the trend of latent heat flux was consistent with that of net radiation until the soil froze in early November. The trends of sensible heat and latent heat had a lot to do with the annual precipitation distribution in the study area. This location's surface flux was dominated by latent heat flux for the whole year, with an annual average of 34.82 W/m2, while sensible heat flux was 26.73 W/m2. There were only two times throughout the year when sensible heat exceeded latent heat: March to May and November to December. According to the trend of the daily average Bowen ratio from January 1st to December 31st, 2014 (Figure 6), it could also be found that the Bowen ratio was larger in the two periods from March to May and from November to December, with a maximum of about 13, and smaller in the rest of the time. As for the daily average soil heat flux, the value was above 0 from mid-March to late August, indicating that the soil heat flux was transmitted from the surface soil to the deep layer, while in other periods, it was negative, which meant soil heat flux was transmitted from the deep layer to the surface. In May, the monthly average soil heat flow peaked. Net radiation had the greatest impact on the trend of soil heat flow, with a correlation coefficient of 0.70 that passed the 99 percent significance test. It could be seen from the figure that in late March, the daily average soil heat flux was abnormally large, which was consistent with the findings of Li et al. (2017) in the research on the variation characteristics of soil heat flux in the Loess Plateau. Actually, this phenomenon was out by soil melting. The soil temperature gradient grew as ice melting into water absorbed heat, increasing the heat flux transported from the surface soil to the deep soil. The yearly average soil heat flux in the research area in 2014 was -1.45 W/m2, indicating that soil heat flux was transported from the deep soil to the surface in 2014.

It can be seen from Figure 6 that the simulation of CLM on the changing trend of surface heat flux is basically consistent with the observed value, and the simulation effect of CLM5.0 is better than that of CLM4.5, especially for net radiation and sensible heat flux. The simulated value of net radiation is generally higher than the observed value, especially in winter, which is mainly due to the high simulated surface long-wave radiation. The simulation results of CLM4.5 for sensible heat flux are relatively low, while CLM5.0 improves the thermodynamic and kinetic roughness parameterization scheme in the model, and the simulation results are close to the observed values. For latent heat flux and soil heat flux of 5 cm, the simulated values of CLM5.0 and CLM4.5 are basically the same and very close to the observed values. In particular, the root mean square errors of soil heat flux of 5 cm are 8.9 W/m$^2$ and 9.9 W/m$^2$, respectively. In general, the CLM model simulates the surface heat flux well. However, neither CLM5.0 nor CLM4.5 can reproduce the process of the abrupt increase in latent heat flux in early January, and the reasons for this need to be explored further.
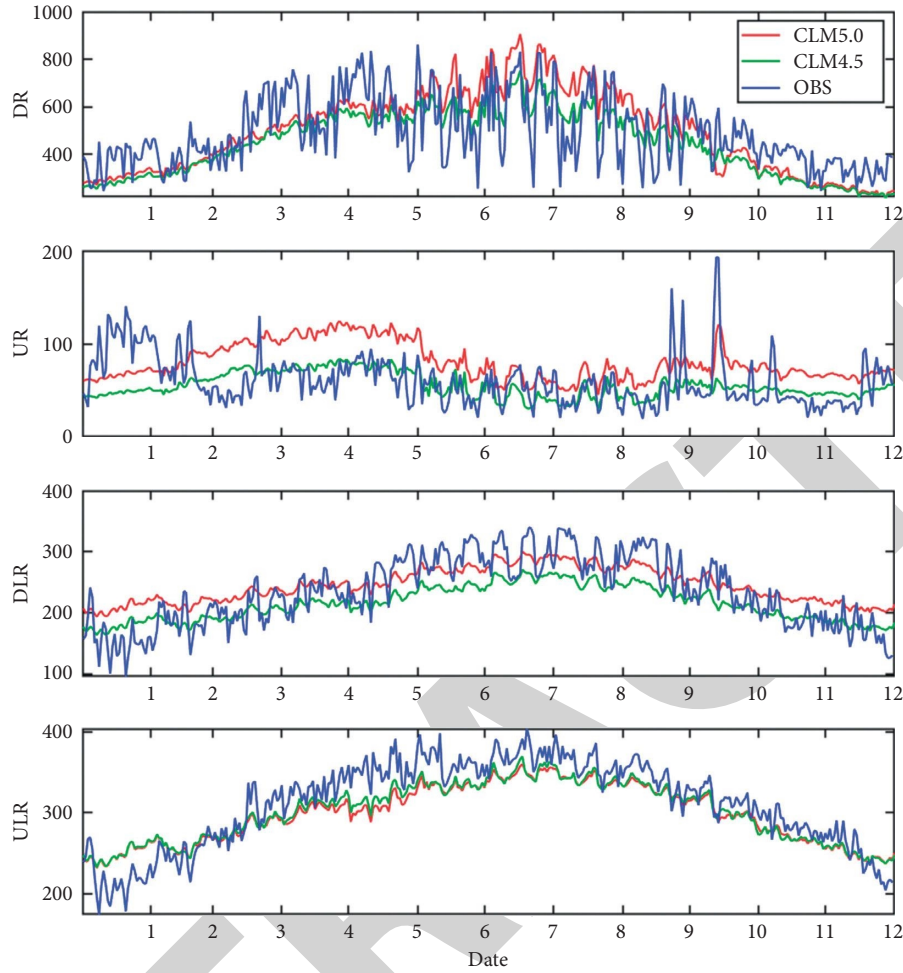
FIGURE 4: Daily average variation of surface radiation at the source region of Yellow River from January 2014 (observed and simulated).

### 3.4. CO₂ Flux.

*3.4. CO$_2$ Flux.* From January 1st to December 31st, 2014, Figure 7 depicts the trend of daily average $CO_2$ flux. During the soil frozen period, the daily average $CO_2$ flux was largely zero, with a little higher variance in two periods from May to mid-June and September to October. In May, September and October, the respiration of alpine meadows dominated, releasing $CO_2$ flux with a daily average of up to 0.23 mg m$^{-2}$ S$^{-1}$ (negative represents absorption and positive emission), while in early June, the photosynthesis of alpine meadows was dominant, absorbing $CO_2$ flux with a daily average of approximately 0.5 mg·m$^{-2}$·S$^{-1}$. In the period from late June to mid-August, when both the moisture and temperature of soil were relatively larger and the vegetation experienced a rapid growth, the daily average $CO_2$ flux increased significantly, with the daily average of $CO_2$ flux absorbed up to 3 mg m$^{-2}$ S$^{-1}$. It was noticeable that in April when the frozen soil melted, the $CO_2$ flux emitted by the surface reached the peak of the year, with the daily average $CO_2$ flux released up to 0.37 mg m$^{-2}$ S$^{-1}$.

Studies have shown that the freeze-thaw areas were important sources of greenhouse gas emission, and the greenhouse gas emitted during the thawing period accounted for a significant share of the total annual emission [15, 16]. Freezing and thawing changing the

physical properties of soil was mainly through their effects on the production and emission of greenhouse gases from two aspects. First, the size and stability of soil aggregates were changed, resulting in the fragmentation of aggregates and the release of a large amount of active organic carbon, which was used by microorganisms and then promoted mineralization and denitrification. Second, a thin coating of ice was applied to the surface of frozen soil particles, reducing soil permeability. Not only was oxygen prevented from entering the soil, resulting in an anaerobic environment ideal for denitrification, but gases created in the soil were also stopped from diffusing outward, accumulating in the soil, and generating an emission peak when the soil melted (Teepe et al., 2001; Koponen et al., 2004). As for the daily variation of $CO_2$ flux in each season (the figure was omitted), when the soil was frozen, for example, in January, the variation of $CO_2$ flux was really slight, generally no daily change, while in April when the frozen soil melted, $CO_2$ was mainly emitted at night, and the maximum of average $CO_2$ flux released in this month was 0.35 mg m$^{-2}$ S$^{-1}$. In addition, there was generally no emission and absorption during the day. Hence the $CO_2$ flux was 0. In the season when surface vegetation grew rapidly, for example, in July, the variation of daily average
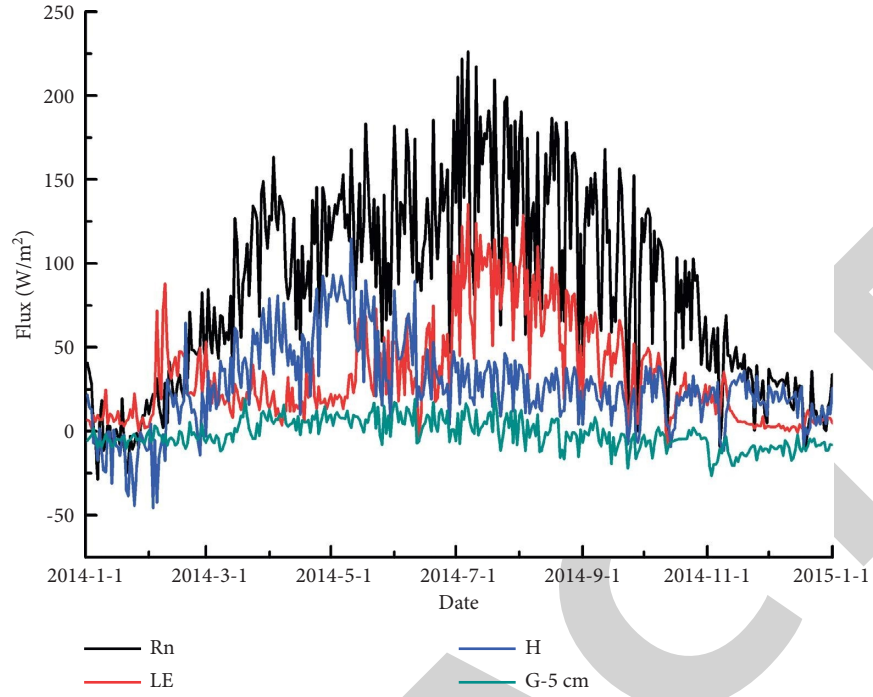
Figure 5: Daily average variation of Surface flux at source region of Yellow River, 2014.
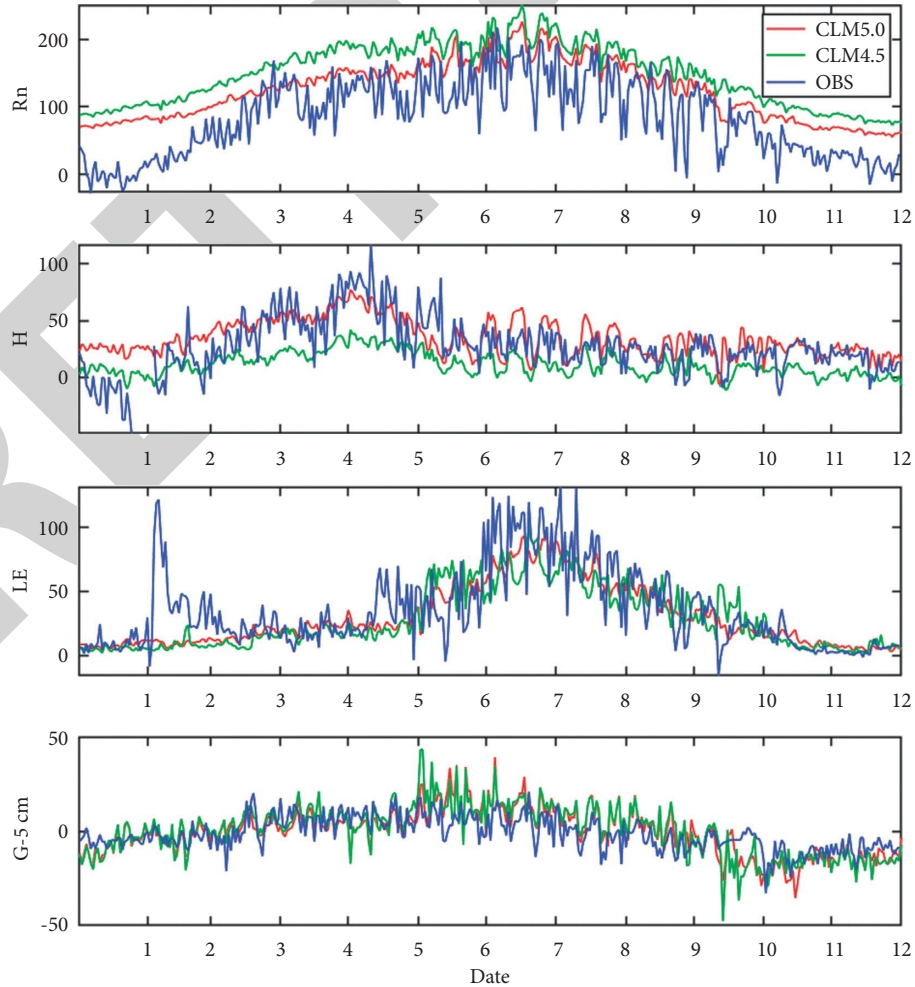


Figure 6: Daily average variation of Surface flux at source region of Yellow River, 2014 (observed and simulated).
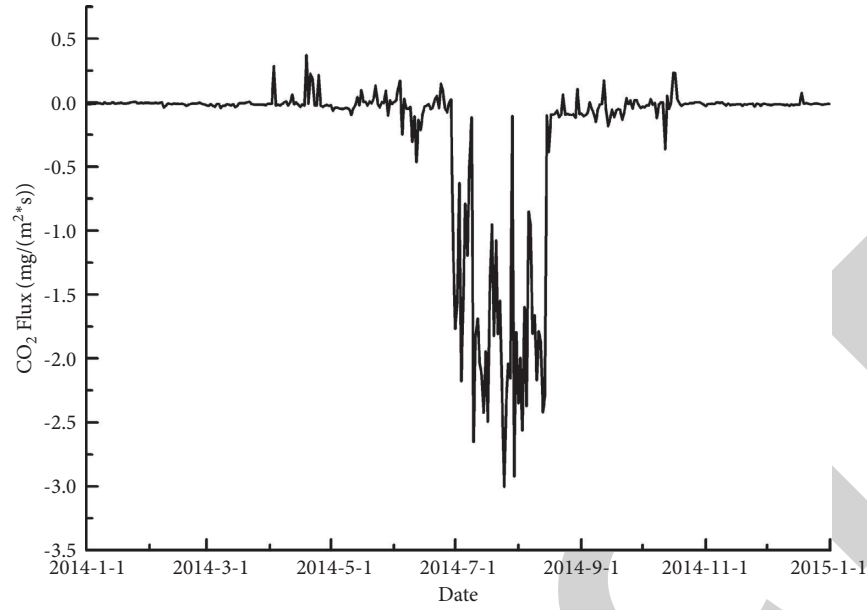
FIGURE 7: Daily average variation of $CO_2$ flux at source region of Yellow River, 2014.

$CO_2$ flux was characterized by the nighttime emission of $CO_2$ due to the respiration, up to $2.47 \, mg \, m^{-2} \, S^{-1}$, and the daytime absorption of $CO_2$ due to the photosynthesis, up to $7.03 \, mg \, m^{-2} \, S^{-1}$. In October, the $CO_2$ released and absorbed by the soil and alpine meadow system were generally the same, making the daily average of $CO_2$ flux almost 0, but the absorption and emission mainly occurred at night, with little change during the day. This indicated that the absorption of $CO_2$ had nothing to do with photosynthesis and may be related to the beginning of soil freezing. That needs further research and verification.

## 4. Conclusions

This paper has conducted research on the various characteristics of surface flux and surface parameters of the alpine meadow underlying surface based on the observation data of Maduo Site at the Yellow River source area in the Qinghai-Tibet Plateau from January 1st to December 31st, 2014. The results are as follows:

(1) The daily average soil temperature of 5 cm depth in the Yellow River source area was negative from January to March, and the soil was frozen during this period, while from early April to mid-October, the daily average soil temperature of 5 cm depth rose to 0°C and above, with the maximum occurring in late July. After mid-October, the daily average soil temperature of 5 cm depth gradually dropped to negative again. During the soil frozen period, the daily average soil moisture at 5 cm depth was lower, with an average volumetric water content of only 0.06. Although there was no freezing from early May to mid-June, the soil moisture was lower until the rainy season arrived in late June, when the soil moisture of 5 cm depth increased significantly, reaching a peak of 0.32. This situation would

continue to late October until the frozen period came in early November, and the soil moisture of 5 cm depth decreased rapidly.

(2) The total radiation in the Yellow River source area was relatively lower in winter, with an average of about $420 \, W/m^2$. It rose rapidly after mid-March, reaching a maximum in June or July, with an average of about $650 \, W/m^2$, and then slowly decreased. The total radiation was mainly affected by the seasonal variation of solar elevation angle. On the other hand, the surface reflected radiation was affected by both total radiation and surface albedo. The short-wave radiation reflected by the surface was often larger in winter and smaller in summer, especially after the rainy season, due to the snow on the surface. Because of the increased soil moisture, the amount of short-wave radiation reflected by the surface was reduced even further. Long-wave surface radiation followed the same seasonal pattern as air counter radiation, with a low point in the winter and a high point in the summer. Besides, the long-wave surface radiation was larger than atmospheric counter radiation. In 2014, the long-wave surface radiation averaged about $311 \, W/m^2$, while the atmospheric counter radiation $234 \, W/m^2$. Due to factors such as cloud cover, the amplitude of daily average atmospheric counter radiation was larger than the daily average of long-wave surface radiation.

(3) The trend of daily average net radiation was similar to that of total radiation, which was rising rapidly after mid-March, reaching a maximum in July, and then decreasing slowly. Net radiation entered the trough in winter, even below 0 in January. The quick increase in daily average net radiation at the beginning of July was due to a drop in surface albedo driven by a sudden increase in soil moisture. In

January, the perceptible heat flux was mainly negative, gradually increasing from February through May, peaking in May, and then gradually declining. The trend of latent heat flux, on the other hand, was substantially different from that of sensible heat flux. In the first six months, when the soil moisture was smaller, the latent heat flux was smaller, too, until early July, when the soil moisture started to rise, and latent heat flux experienced rapid growth along with it.

Before July, the trend of sensible heat was consistent with that of net radiation, while after July, the trend of latent heat flux was consistent with that of net radiation until the soil was frozen in early November. This trend of sensible heat and latent heat had a lot to do with the annual precipitation distribution in the study area. For the whole year, the surface flux of the study area was dominated by latent heat flux, with an annual average of $34.82 \, \text{W/m}^2$, while the annual average of sensible heat was $26.73 \, \text{W/m}^2$. The daily average of soil heat flux was above 0 from mid-March to late August, soil heat flux transmitted from the surface soil to the deep layer, while the rest of the time below 0, soil heat flux transmitted from the deep layer to the surface soil. The monthly average of soil heat flux reached a peak in May. Net radiation influenced the trend of soil heat flow the most, and the correlation coefficient between the two was 0.70, passing the 99 percent significance test. The soil heat flux showed an extremely significant daily average in late March, which was linked to the melting of frozen soil. The average soil heat flux in the study area was $-1.45 \, \text{W/m}^2$ in 2014, indicating that in this area and in this year, soil heat flux was transmitted from the deep layer to the surface soil.

(4) The simulation results of CLM5.0 and CLM4.5 for soil temperature and humidity at Maduo site are general, especially in the period of soil freezing and thawing in winter. For radiation flux and surface heat flux, the simulation results of CLM 5.0 and CLM 4.5 are much better, especially CLM 5.0. The simulation findings are quite similar to the observed values, indicating that the model's simulation effect in the alpine grassland of the Yellow River's source region has been greatly enhanced after several parameterization schemes and dynamic processes were improved. However, the soil freezing and thawing process and snow parameterization scheme in CLM need to be further improved.

(5) During the soil frozen period, the daily average $CO_2$ flow in the Yellow River source area was normally 0; however, the daily average $CO_2$ flux varied greatly between May and June and September and October. Specifically, in May, September, and October, the respiration of alpine meadows was dominant, with the daily average CO2 flux released up to $0.23 \, \text{mg} \cdot \text{m}^{-2} \bullet \text{s}^{-1}$, and in early and mid-June, the

photosynthesis of alpine meadows played the leading role, absorbing $CO_2$ flux with a daily average of close to $0.5 \, \text{mg} \cdot \text{m}^{-2} \bullet \text{s}^{-1}$. In the period from late June to mid-August, when both the moisture and temperature of soil were relatively larger, the surface vegetation experienced rapid growth and the daily average $CO_2$ flux significantly increased, with the maximum of daily average $CO_2$ flux absorbed up to $3 \, \text{mg} \cdot \text{m}^{-2} \bullet \text{s}^{-1}$. During the thawing period in April, the $CO_2$ flux emitted by the surface reached the peak of the year, and the daily average $CO_2$ flux released by the soil was up to $0.37 \, \text{mg} \cdot \text{m}^{-2} \bullet \text{s}^{-1}$. When the soil was frozen, generally there was no daily change in $CO_2$ flux. In April, as the frozen soil melted, $CO_2$ emission only occurred at night, and generally there was no emission and absorption during the day. In July, when the surface vegetation grew vigorously, the daily change of average $CO_2$ flux was represented as the nighttime emission of $CO_2$ due to the respiration, up to $2.47 \, \text{mg} \cdot \text{m}^{-2} \bullet \text{s}^{-1}$, and the daytime absorption of $CO_2$ due to the photosynthesis, up to $7.03 \, \text{mg} \cdot \text{m}^{-2} \bullet \text{s}^{-1}$. The $CO_2$ emitted and absorbed by the soil and alpine meadow system were usually the same in October, with the daily average $CO_2$ flow mostly 0; however, absorption and emission primarily happened at night, with little variation during the day. This revealed that $CO_2$ flow absorption was unrelated to photosynthesis and could be linked to the onset of soil freezing. That necessitates more investigation and verification.

## Data Availability

The datasets used during the current study are available from the corresponding author upon reasonable request.

## Conflicts of Interest

The authors declare that they have no conflicts of interest.

## Acknowledgments

## References

[1] R. Dickison, "Land-atmosphere interaction," *U.S. Nation report inter-nation Union of Geology and Geophysics Sciences*, vol. 33, pp. 917–922, 1995.

[2] A. Henderdon-Sellers, "The project of inter-comparison of land surface parameterization schemes," *Bull. AmerSoc*, vol. 74, no. 7, pp. 1335–1348, 1993.

[3] S. F. Sun, *Parameterization Study of Physical and Biochemical Mechanism in Land Surface Process*, Meteorology Press 1-3, Beijing China, 2005.

[4] B. G. Heusinkveld, J. Afg, H. Aam, and S. M. Berkowicz, "Surface energy balance closure in an arid region: role of soil

heat flux," *Agricultural and Forest Meteorology*, vol. 122, no. 1–2, pp. 21–37, 2004.

[5] L. Gu, J. Yao, Z. Hu, and L. Zhao, "Comparison of the surface energy budget between regions of seasonally frozen ground and permafrost on the Tibetan plateau," *Atmospheric Research*, vol. 153, pp. 553–564, 2015.

[6] Z.-c. Li, Z.-g. Wei, S.-h. Lv et al., "Effect of land surface processes on the Tibetan Plateau's past and its predicted response to global warming: an analytical investigation based on simulation results from the CMIP5 model," *Environmental Earth Sciences*, vol. 72, no. 4, pp. 1155–1166, 2014.

[7] K. Tanaka, H. Ishikawa, T. Hayashi, I. Tamagawa, and Y. M. Ma, "Surface energy budget at amdo on the Tibetan plateau using game/tibet iop98 data," *Journal of the Meteorological Society of Japan*, vol. 79, no. 2, pp. 181–189, 2001.

[8] J. Yao, L. Zhao, L. Gu, Y. Qiao, and K. Jiao, "The surface energy budget in the permafrost region of the Tibetan plateau," *Atmospheric Research*, vol. 102, no. 4, pp. 394–407, 2011.

[9] S. B. Idso, R. D. Jackson, R. J. Reginato, B. A. Kimball, and F. S. Nakayama, "The dependence of bare soil albedo on soil water content," *Journal of Applied Meteorology*, vol. 14, no. 1, pp. 109–113, 1975.

[10] H. T. Koponen, L. Flöjt, and P. J. Martikainen, "Nitrous oxide emissions from agricultural soils at low temperatures: a laboratory microcosm study," *Soil Biology and Biochemistry*, vol. 36, no. 5, pp. 757–766, 2004.

[11] Z. Li, J. Yang, Z. Zheng et al., "Comparative study of the soil thermal regime in arid and semi-humid areas," *Environmental Earth Sciences*, vol. 76, no. 1, p. 28, 2017.

[12] P. T. Morkved, P. Dorsch, T. M. Henriksen, and L. R. Bakken, "N2O emissions and product ratios of nitrification and denitrification as affected by freezing and thawing," *Soil Biology and Biochemistry*, vol. 38, no. 12, pp. 3411–3420, 2006.

[13] C. D. Peter- Lidard, E. Blackburm, X. Liang, and E. F. Wood, "The effect of soil thermal conductivity parameterization on surface energy fluxes and temperature," *Journal of the Atmospheric Sciences*, vol. 55, no. 7, pp. 1209–1224, 1998.

[14] M. S. Roxy, V. B. Sumithranand, and G. Renuka, "Variability of soil moisture and its relationship with surface albedo and soil thermal diffusivity at astronomical observatory, Thiruvananthapuram, south Kerala," *Journal of Earth System Science*, vol. 119, no. 4, pp. 507–517, 2010.

[15] R. Teepe, R. Brumme, and F. Beese, "Nitrous oxide emissions from soil during freezing and thawing periods," *Soil Biology and Biochemistry*, vol. 33, no. 9, pp. 1269–1275, 2001.

[16] X. Wu, N. Brüggemann, R. Gasche, Z. Shen, B. Wolf, and K. Butterbach-Bahl, "Environmental controls over soil-atmosphere exchange of N2O, NO, and CO2in a temperate Norway spruce forest," *Global Biogeochemical Cycles*, vol. 24, no. 2, pp. a–n, 2010.